HHS Public Access

Author manuscript

Anal Chem. Author manuscript; available in PMC 2022 July 16.

Published in final edited form as:

Anal Chem. 2021 August 10; 93(31): 10990–10998. doi:10.1021/acs.analchem.1c02163.

Multidimensional Separations of Intact Phase II Steroid Metabolites Utilizing LC-Ion Mobility-MS

Don E. Davis Jr.[1], **Katrina L. Leaptrot**[1], **David C. Koomen**[1], **Jody C. May**[1], **Gustavo de A. Cavalcanti**[2], **Monica C. Padilha**[2], **Henrique M.G. Pereira**[2], **John A. McLean**[1]

[1]Department of Chemistry, Center for Innovative Technology, Institute of Chemical Biology, Institute for Integrative Biosystems Research and Education, Vanderbilt-Ingram Cancer Center, Vanderbilt University, Nashville, Tennessee, United States

[2]Brazilian Doping Control Laboratory– LBCD – Chemistry Institute – Federal University of Rio de Janeiro – UFRJ, Rio de Janeiro, RJ, Brazil

Abstract

The detection and unambiguous identification of anabolic-androgenic steroid metabolites are essential in clinical, forensic, and anti-doping analyses. Recently, sulfate phase II steroid metabolites have received increased attention in steroid metabolism and drug testing. In large part, this is because phase II steroid metabolites are excreted for an extended time, making them a potential long-term chemical marker of choice for tracking steroid misuse in sports. Comprehensive analytical methods, such as liquid chromatography-tandem mass spectrometry (LC-MS/MS), have been used to detect and identify glucuronide and sulfate steroids in human urine with high sensitivity and reliability. However, LC-MS/MS identification strategies can be hindered by the fact that phase II steroid metabolites generate non-selective ion fragments across the different metabolite markers, limiting the confidence in metabolite identifications that rely on exact mass measurement and MS/MS information. Additionally, liquid chromatography-high resolution mass spectrometry (LC-MS/MS (HRMS)) is sometimes insufficient at fully resolving the analyte peaks from the sample matrix (commonly urine) chemical noise, further complicating accurate identification efforts. Therefore, we developed a liquid chromatography-ion mobility-mass spectrometry (LC-IM-MS) method to increase the peak capacity and utilize the IM-derived collision cross section (CCS) values as an additional molecular descriptor for increased selectivity and improve identifications of intact steroid analyses at low concentrations.

Graphical abstract

*Corresponding Author john.a.mclean@vanderbilt.edu.

Author Contributions

Experimental design and conceptualization were performed through contributions by all authors. This manuscript was written through contributions of all authors, each who have given approval to the final version of the manuscript.

Supporting Information.

The Supporting Information is available free of charge on the ACS Publications website at DOI:

Supporting Information: LC-IM-MS instrument settings, and data presented in this work.

The authors declare no competing financial interest.

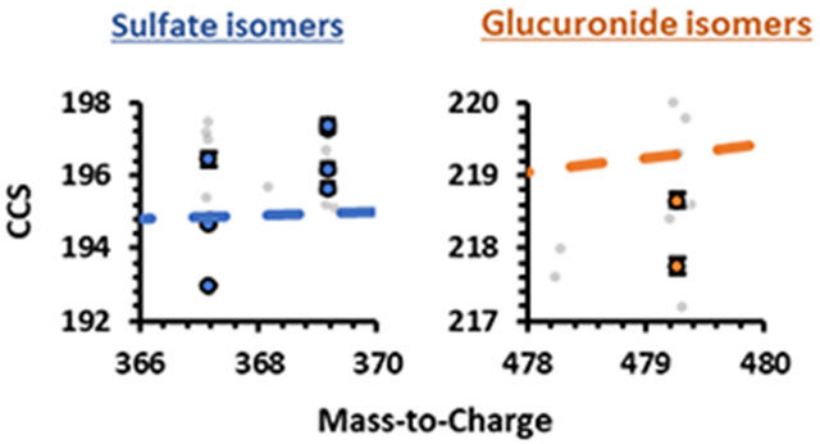

Exogenous anabolic-androgenic steroids (AASs) are performance enhancement drugs obtained by structural modifications of testosterone. AASs are the most reported prohibited substances in competitive sports.[1–4] Urine sampling is the matrix of choice for testing the presence of AAS because many steroid metabolites are eliminated through urine. AAS metabolites exhibit a slow elimination rate in the urinary system, allowing drug testing laboratories to detect them over an extended period following exposure. Furthermore, urine is a non-invasive sample collection strategy. Usually, AASs undergo two phases of enzyme-controlled metabolism to inactivate the drug and facilitate its elimination from the body via the bioconversion of AAS into more hydrophilic compounds.[1] Phase I reactions mainly include oxidation and reduction, making the compounds more suitable for subsequent phase II reactions. The most common phase II reactions are conjugations with sulfonic acid and glucuronic acid.[1,5,6]

Routine analyses of AAS metabolites often use indirect methods such as hydrolysis of phase II metabolites, followed by liquid-liquid extraction and derivatization reactions for increased volatility and thermal stability for GC-MS/MS detection.[1,7] Sensitivity challenges in atmospheric pressure ionization (API) methods have been extensively described for the aglycone counterparts of AASs.[8,9] Thus, the sensitivity required in drug testing is difficult to achieve. More recent work has demonstrated that AAS phase II metabolites can be analyzed directly via LC-MS/MS due to their moderate acidity.[1,10–13] LC-MS/MS has been shown to be suitable for determining the presence of hydrolysis resistant glucuronide metabolites.[14] Nevertheless, this approach does not provide intact steroid structural characterization, relying instead on unspecific fragment ions observed in the MS2 spectra. Derivatization reactions are also sometimes used for LC-MS/MS analyses to address ionization issues. However, the sample preparation for derivatization reactions is time-consuming and can yield multiple derivative products.[15]

Despite these challenges, the best targets to track AAS misuse in sports are those eliminated in urine over extended time periods. These are usually referred to as AAS long-term metabolites (LTMs). These LTMs were a turning point in AASs characterization through expanding the detection window of AASs in anti-doping analyses.[1,16] Discovering novel LTMs of AAS with improved analytical capabilities has led to significant improvements

in anti-doping scenarios.[1,16–21] For example, dehydrochloromethyltestosterone's (DHCMT) estimated detection window without its LTM is 8-18 days, but through inclusion of its LTM this window can be expanded to *ca.* 250 days.[16,17,19–21]

Recently, new LTMs have been described in the sulfate fraction, but current analytical methods cannot detect these metabolites in a high-throughput manner. Exhaustive and inefficient chemical hydrolysis reactions are required to detect the desirable non-sulfated derivative for MS analyses.[22] GC-MS/MS analyses have been utilized for detecting the sulfate metabolites to avoid the inconveniences described above. The degradation products of non-hydrolyzed sulfated metabolites are detected, instead.[23] This approach is not reliable since these degradation products are generated in the GC injection port, and are difficult to control.

A further analytical challenge in detecting AAS metabolites is that their chemical and isomeric diversity results in numerous isobaric peaks in LC-MS/MS (HRMS) analyses, especially considering the high occurrence of coeluting endogenous interferences in human urine.[24,25] To date, several different analytical strategies have been utilized to characterize AAS and related metabolites.[11,16–20,22,23,26–35] Traditionally, these techniques consist of GC-MS/MS, LC-MS/MS, and/or LC-MS/MS (HRMS). However, inherent issues are apparent with intact phase II steroid metabolites selectivity due to poor fragmentation in API sources and tandem mass spectrometry described by previous studies.[15,24,36] More selective and sensitive analytical methods that are capable of addressing sample complexity and throughput are needed in doping control laboratories to discover novel markers and address the ongoing misuse of AASs.[6,16,37]

Ion mobility spectrometry (IMS) is a gas-phase separation technique that distinguishes ions based on their size, shape, and charge state.[38–66] The IMS size and shape measurement takes the form of an ion collision cross section (CCS), which is a coarse-grained surface area measurement (reported in square angstroms, $Å^2$) encompassing the ion size as well as its interaction with the neutral gas. IMS separates ions based on differences in gas phase electrophoretic mobility, while in contrast, GC and LC separations are primarily based on differences in analyte boiling point\vapor pressure and polarity, respectively. Gas-phase IMS analyses are rapid, typically occurring on a time scale of 10-100 ms per spectrum, whereas condensed phase LC-MS is on the time scale of minutes. Therefore, IMS can be included in existing LC-MS workflows without compromising analytical throughput, providing an additional separation dimension and an associated molecular descriptor (CCS) to support analyte detection and identification.[38,50] Previously, IMS has been utilized to characterize intact AASs along with their phase I and phase II metabolites.[24,54,67–72] Various IMS techniques, such as field asymmetric IMS (FAIMS), traveling wave IMS (TWIMS), and drift tube IMS (DTIMS), have been utilized for AAS analyses.[50,67–74] The Yost research group investigated the effect of Group 1 cation adducts on resolving AAS isomers using FAIMS, providing direct separation of metal-coordinated AAS isomers with no increase in analysis time or modifications to the instrumentation, which is useful for high-throughput screening.[71] Hernández-Mesa et al. have successfully cross-validated the first TWIMS database for steroids in calve urine and obtained CCS values within 2% of literature databases entries.[68] The Chouinard group has demonstrated the application of the

Paternò-Büchi reaction for structural modification of steroid isomers, prompting improved identification by DTIMS, which is promising due to the simplicity, low cost, and relatively high efficiency of the Paternò-Büchi reaction for generating structurally-informative ions.[67]

Online, multidimensional analytical separations such as liquid chromatography-ion mobility-mass spectrometry (LC-IM-MS) may be necessary for AAS analyses, particularly for complex human sample matrices where numerous isobaric and isomeric compounds (e.g., nominal mass interferents and analyte structural isomers) are commonly encountered.[24,57,75] In addition to LC-MS/MS (HRMS) and GC-MS/MS, LC-IM-MS has become an essential analytical technique for characterizing metabolites simultaneously by molecular structure and weight.[49,52,63,66,75–77]

In this work, we describe an LC-IM-MS workflow based on DTIMS that supports anti-doping efforts to improve the detection of relevant,endogenous, and long-term intact AAS phase II metabolites in human urine at low concentrations. Collision cross section (CCS) values derived from DTIMS analysis show utility in improving the confidence in assigning small-molecule AAS identifications. The combined LC-IM-MS workflow described here delivers reliable and accurate qualitative results for AAS phase II metabolites and should prove beneficial for laboratories interested in increasing efficiency and accuracy in anti-doping analyses.

Experimental Methods

Standards and Chemicals.

Steroids utilized in this study are presented in Table 1. Epitestosterone S (4-androsten-17α-ol-3-one sulphate), 7-Keto DHEA-3 S (5-androsten-3β-ol-7,17-dione sulphate), 16α-hydroxy DHEA S (5-androsten-3β, 16α-diol-17-one-3 sulphate), Prednisolone 21-S (1,4-pregnadien-11,17,21-triol-3,20-dione 21-sulphate), 11-Ketoetiocholanolone S (5β-androstan-3α-ol-11,17-dione sulphate), Prasterone S (3β) (5-androsten-3β-OL-17-one sulphate), Epiandrosterone S (5α-androstan-3β-ol-17-one sulphate), Prasterone (3α) S (5-androsten-3α-OL-17-one sulphate), 5α-androstan-3β-ol-one S, Etiocholanolone S (5β-androstan-3α-ol-17-one sulphate), and Androsterone S (5α-androstan-3α-ol-17-one sulphate) were purchased from Steraloids Inc. (Newport, RI, USA). Drostanolone M1 G (2α-methyl-5α-androstan-3α-ol-17-one-3-β-D-glucuronic acid), Methenolone M1 G (1-methylene-5α-androstan-3α-ol-17-one-3-β-D-glucuronic acid), Mesterolone M1 G (1α-methyl-5α-androstan-3α-ol-17-one-3β-D-glucuronic acid), Mesterolone M2 G (1α-methyl-5α-androstan-3α,17β-diol-3-β-D-glucuronic acid), Boldenone G (1,4-adrostadien-17β-diol-3-one-17-β-D-glucuronic acid), Bolasterone M1 G (7α,17α-dimethyl-5β-androstan-3α,17β-diol-3-β-D-glucuronic acid), Stanozolol 3'OH G (5α-androstan-[3,2-c] pyrazole-3',17β-diol-17α-methyl-3'-β-glucuronic acid, Nandrolone G (4-estren-17β-ol-3-one-17-β-D-glucuronic acid), Epinandrolone S (17α-sulfoxy-4-estren-3-one), 19-norandrosterone D4 G (2,2,4,4-d4-5α-Estran-3α-ol-17-one-3-β-D- glucuronic acid), Testosterone D3 S (16,16,17α-d3-17β-sulfoxy-androst-4-en-3-one) were purchased from The National Measurement Institute of Australia (NMIA). Epi-THMT S3 (3α-sulfoxy-17β-methyl-5β-androstan-17α-ol) was a kind gift from the Institute Hospital del Mar d'Investigacions Mèdiques (IMIM) (Barcelona, Spain). Stanozolol 1'N-G (5α-

androstan-[3,2-c] pyrazole-3',17β-diol-17α-methyl-1Ń-glucuronic acid) was provided by Seibersdorf Laboratories (Austria). All 22 AAS chemical structures are shown in Figure 1, with sections depicting constitutional isomer and stereoisomer groups along with CCS values for interday (n = 3 technical replicates over 3 different days) analyses in this study. Optima LC/MS grade water, methanol, formic acid, and ammonium formate were obtained from Fisher Scientific (Hampton, NH, USA).

Human Urine Extraction and Preparation.

Solid-phase extraction (SPE-C_{18} Cartridges) was used for all urine samples. Briefly, 2 mL of methanol and 2 mL of water were used for cartridge conditioning. Afterward, the cartridge was loaded with 5 mL of each human urine sample. Next, the cartridges were washed with 10% methanol in water. Then, the steroid metabolites were eluted with 100% methanol, andthe solvent was evaporated under a nitrogen stream at 40 °C for 40 min. The final extract was reconstituted with 100 μL of mobile phase buffer before analyses.

Chromatographic Conditions.

For the LC-IM-MS method, steroid standards were analyzed using a 2.1 x 75 mm (1.7 μm) reversed-phase column, Waters ACQUITY BEH C18 (Waters Corporation, Milford, MA) with a 2.1 x 5 mm 1.7 μm Waters ACQUITY BEH C18 Vanguard precolumn (Waters Corporation, Milford, MA), maintained at 45 °C for separation by Ultra High-Pressure Liquid Chromatography (UHPLC, Agilent 1290 Infinity I system, Agilent Technologies, Santa Clara, CA). Mobile phase A consisted of water with 0.1% formic acid and 1 mM ammonium formate. Mobile Phase B consisted of methanol with 0.1% formic acid and 1 mM ammonium formate. The UHPLC was directly coupled online to a commercial DTIMS-MS (6560, Agilent). A 10 μL sample was injected at a flow rate of 400 μL/min and was analyzed using the following chromatographic conditions (15 minute total runtime including purge and equilibration times): mobile phase B was maintained at 45% for the first 1 minute for an initial isocratic hold, linearly increased from 45% to 70% over 8.5 minutes, linearly increased again from 70% to 100% over 1 minute, and held at 100% for 1.5 minutes. Mobile phase B returned to 45% by 13 minutes and was held at 45% for 2 minutes to re-equilibrate the column. A shorter 10 minute LC method was used for human urine samples to increase throughput (Table S1). In these methods, the initial isocratic hold, final purge, and re-equilibration times were performed to ensure efficient cleaning, minimize carryover, and preserve column integrity.

DTIMS-MS conditions.

AASs were analyzed in negative ionization mode using the Jet Stream ESI source (Agilent) coupled with a drift tube ion mobility mass spectrometer (6560, Agilent) using settings similar to previously described instrumental methods.[38,44,46,47,50,78] Ionization source conditions were optimized (e.g., gas temperature, drying gas, nebulizer pressure, sheath gas temperature, sheath gas flow, capillary voltage, and nozzle voltage in Table S1) for flow injection analysis (FIA) to maximize sensitivity. The IM analyses used nitrogen drift gas with the drift tube at a temperature of 30 °C, a pressure of 4.0 Torr, and an electric field of 17.3 V/cm. A single field CCS method was used to determine CCS values via a modified Mason-Schamp equation.[46] Data were acquired using MassHunter Workstation

Data Acquisition software (Agilent) and analyzed using MassHunter Qualitative Analysis (Agilent), MassHunter IM-MS Browser (Agilent), and Skyline (MacCoss Lab).[79,80] Statistical analyses for isomeric AAS phase II metabolite RT and CCS measurements were performed using GraphPad Prism (version 8.0). Significant difference was assessed based on a p-value < 0.05 from appropriate statistical tests (t-tests (Tables S2–S3) and one-way analysis of variance (ANOVA) tests (Tables S4–S5)).

Results and Discussion

LC-IM-HRMS.

The data in Figure 2 was extracted for Epi-THMT S3 (*m/z* 367.194), which had the same LC retention time in the pure standard, the standard spiked in urine, and the urine blank samples (panel A). Panel B showed that the peak arising from the urine blank was an interference because the CCS percent error between the pure standard and the urine blank was > 5%. On the other hand, the CCS percent error between the pure standard and standard spiked in urine was ~0.5%, which is within the margin of error for DTIMS (panel B). Panel C demonstrates how HRMS alone could not fully resolve the masses for Epi-THMT S3 and the interference. However, when data filtering is used in the DTIMS dimension, the interference can be resolved from Epi-THMT S3 (LC-IM-MS).

To evaluate the selectivity and applicability of the DTIMS dimension in analyzing AASs, Figure 3 exhibits the theoretical isotope distribution patterns for Epi-THMT S3, Drostanolone M1 G, and Stanozolol 1'N – G. Theoretical isotopic distribution patterns were compared to the extracted mass spectra of the (1) MS only, (2) LC-MS, (3) IM-MS, and (4) LC-IM-MS dimensions which were analyzed from human urine samples. These data collectively illustrate that information derived from the multiple separation dimensions, particularly IM-derived CCS values, contribute increased selectivity and analyte identification assurance. For all three AASs, the LC-IM-MS analyses distinctively resolved coexisting interferences and enhanced certainty in AAS differentiation. Lastly, Figure 3 demonstrates the utility of the IM dimension to resolve concomitant species from human urine that were not separated in the LC or HRMS dimensions alone.

A representative CCS vs. retention time plot of the 22 AAS IMS and LC profiles is shown in Figure 4C. Table 1 also denotes AAS formulas, exact masses, isomer groups, $[M-H]^-$ measured masses, retention times (RT), RT coefficient of variations (CV%), CCS, and CCS CV%. Additionally, CCS and *m/z* correlations are shown in Figure S2 and Figure S3. These data collectively demonstrate the structural diversity among the AAS phase II steroids outlined in this study even though there are many isomer groups (Table 1 and Figure 1). Chromatographically, most isomeric AASs were shown to display statistically significant separations with some overlapping retention times (based on CV% in Table 1, standard error bars in Figure 4A, and p-values in Table S2–S5). For most isomeric AASs that did not exhibit statistically significant separation chromatographically, the data show that there were statistically significant CCS values (difference based on standard error bars in Figure 4 and p-values in Table S2–S5). By combining LC, IM, and MS data, all AASs examined, except for Etiocholanolone S and Androsterone S, were statistically significant and separated in

either chromatography, ion mobility, or mass spectrometry dimensions (font colors represent AAS isomers in Table 1, Figure 1, Figure 4, and p-values in Table S2–S5).

Isomer Separation.

To assess the utility of the LC-IM-MS method for separating isomeric AASs (Table 1, Figure 1, Figure 4, Figure S4, and Table S2–S5), we analyzed 11 analytes belonging to 4 isomeric sets including 16α-hydroxy DHEA 3-S (in blue), 11-ketoetiocholoanolone S (in blue), Prasterone S (3β) (in green), Epitestosterone S (in green), Prasterone S (3α) (in green), Epiandrosterone S (in gold), 5α-androstan-3β-ol-16-one S (in gold), Etiocholanolone S (in gold), Androsterone S (in gold), Mesterolone M1 G (in orange), and Drostanolone M1 G (in orange). Because isomers have the same chemical formula, this presents challenges for mass separation alone. However, LC-IM-MS analyses give the most accurate results (Figure 3). In the IM dimension, statistically significant separations were readily obtained for all isomer sets except for Epiandrosterone S vs. 5α-androstan-3β-ol-16-one S and Etiocholanolone S vs. Androsterone S (difference based on standard error bars in Figure 4C, Figure S2, Figure S3, and p-values in Table S5). The IMS single-peak resolving power (R_p) values and FWHM peak widths for Epiandrosterone S were ~40.2 and ~0.68 ms, respectively. The IMS R_p values and FWHM peak widths for 5α-androstan-3β-ol-16-one S were ~42.3 and ~0.65 ms, respectively (p-value = 0.92 when CCS values are compared to each other). For the other set of isomers denoted with gold, the IMS single-peak resolving power (R_p) values and FWHM peak widths for Etiocholanolone S were ~48.8 and ~0.56 ms, respectively. The IMS R_p values and FWHM peak widths for Androsterone S were ~47.7 and ~0.57 ms, respectively (p-value = 0.13 when CCS values are compared to each other). These four endogenous AAS phase II metabolite isomers are challenging to differentiate using the current IMS technology and thus would benefit from high resolution IMS techniques such as extended path-length traveling wave IMS (cyclic TWIMS), Structures for Lossless Ion Manipulation (SLIM), trapped IMS (TIMS), FAIMS, or ion multiplexing using DTIMS.[81–86]

Structural analyses of the stereoisomers (in green, Table 1 and Figure 1), Prasterone S (3α), and Prasterone S (3β) along with their constitutional isomer, Epitestosterone S, yielded statistically significant CCS values from each other (in green, difference based on standard error bars in Figure 4C and p-values in Table S4). However, Prasterone S (3β) did not yield statistically significant RT values when compared to Epitestosterone S, but all other RT values were statistically significant (in green, difference based on standard error bars in Figure 4C and p-values in Table S4). The stereoisomers structural analysis (in gold, Table 1), Epiandrosterone S, Etiocholanolone S, and Androsterone S do not all have statistically significant RT values, and these three isomers do not have statistically significant CCS values (in gold, difference based on standard error bars in Figure 4, Figure S2, Figure S3, and p-values in Table S5). The constitutional isomer, 5-α-androstan-3β-ol-16-one S, yielded statistically significant RT values but not CCS values when compared to Epiandrosterone S (in gold, difference based on standard error bars in Figure 4C, Figure S2, Figure S3, and p-values in Table S5). Etiocholanolone S did not yield statistically significant RT and CCS values when compared to Androsterone S (in gold, difference based on p-values in Table S5). Each of the constitutional isomer sets (in blue and orange, Table 1), 16α-hydroxy

DHEA 3-S (in blue), 11-ketoetiocholanolone S (in blue), Mesterolone M1 G (in orange), and Drostanolone M1 G (in orange) all have statistically significant RT and CCS values (difference based on standard error bars in Figure 4C and p-values in Table S2–S3).

Enhancement in AAS Detection Utilizing Ion Mobility.

Sulfate and glucuronide AAS phase II metabolites were detected using both RT and CCS values to examine the complementary separation of each dimension (Figure 4C). There was no consistent trend in the LC elution order as both sulfate and glucuronide AAS phase II metabolites eluted at different times throughout the chromatographic method. However, in the IMS analyses, the CCS values of the sulfate metabolites are smaller than the glucuronide metabolites. By combining approaches, all the isomers (except for Etiocholanolone S and Androsterone S) can be resolved cooperatively using LC-IM-MS.

This study has four isomeric groups consisting of both constitutional isomers and stereoisomers analyzed individually and in a mixture. The LC and IMS separations in Figure 4 (also Table S2–S5) illustrate the power of orthogonal separation mechanisms of polarity (LC) and molecular size in the gas phase (IM). Although not all the isomeric AAS phase II metabolites could be resolved by the LC or MS dimension alone, coupling these two techniques provide a more comprehensive example of isomer separation in 3-dimensional space (LC-IM-HRMS). Once the utility of endogenous steroid sulfates are also demonstrated as a means of identifying suspicious samples arising from pseudo endogenous intaking, the LC-IM-HRMS workflow developed in this study may be quite useful for overcoming selectivity issues found in the conventional LC-MS/MS approach.[87] Furthermore, faster LC gradients can be explored without significantly compromising the LC separation. Fast LC can provide a considerable advantage as it enables analytical results to be achieved more quickly, which is particularly important in major competitive events such as the Olympic Games since the time frame to report the analytical results is necessarily short.

Conclusions

The increase in positive tests reported by WADA accredited laboratories have necessitated the evaluation of new analytical methods that are fit for purpose with regard to analyzing AASs in human urine. This motivation for evaluating new technologies is in response to targeting long-term metabolites of steroids with improved analytical selectivity and sensitivity which ultimately results in a significant increase in positive tests.[16] The lack of high analytical selectivity and sensitivity can complicate accurate identifications in anti-doping analyses.

This manuscript investigates the utility of LC-IM-HRMS analytical workflows in anti-doping applications, which are motivated by inherent limitations with steroid selectivity due to limited diagnostic fragmentation in MS/MS workflows, especially when differentiating isomers. Our analyses provide qualitative measurements of intact phase II metabolite groups (sulfate and glucuronide metabolites). Taken together, 20 out of 22 AASs evaluated in this study (including isomeric species but excluding Etiocholanolone S and Androsterone S) were separated with statical significance when the combined LC-IM-MS analytical

approach was utilized. Additional confidence was gained when matching the CCS values of the tentative steroid identifications (obtained via accurate mass measurement), with CCS measurements from the analytical standards. For the future, CCS predictions using machine learning algorithms will be necessary to populate the numerous possible AAS CCS values for unknown detectionwith high speed and accuracy (e.g., DeepCCS, SIFTER).[88,89] Also, high resolution ion mobility will provide additional selectivity and differentiation needs for AAS analyses that would ultimately lead to higher precision and accuracy for anti-doping applications.[81–86]

Supplementary Material

Refer to Web version on PubMed Central for supplementary material.

ACKNOWLEDGMENT

We would like to thank Stacy D. Sherrod, Nadjali A. Chung, Bailey S. Rose, and Amelia L. Taylor for contributions in various stages with their technical expertise and advice. Financial support for aspects of this research was provided by The National Institutes of Health (National Cancer Institute R03CA222452). Financial support was also provided by Partnership for Clean Competition (PCC) (Grant number #68049MG20) and in part using the resources of the Center for Innovative Technology at Vanderbilt University.

References

(1). Stojanovic BJ; Göschl L; Forsdahl G; Günter G Metabolism of Steroids and Sport Drug Testing. Bioanalysis. 2020, 12 (9), 561–563. 10.4155/bio-2020-0077 [PubMed: 32412346]

(2). Parr MK; Flenker U; Schänzer W The Assay of Endogenous and Exogenous Anabolic Androgenic Steroids. Hormone Use and Abuse by Athletes. 2011, 121–130.10.1007/978-1-4419-7014-5_13

(3). World Anti-Doping Agency (WADA) International Standard Prohibited List 2021 https://www.wada-ama.org/sites/default/files/resources/files/2021list_en.pdf

(4). World Anti-Doping Agency (WADA) World Anti-Doping Code 2021 https://www.wada-ama.org/sites/default/files/resources/files/2021_wada_code.pdf

(5). Gómez C; Pozo OJ; Marcos J; Segura J; Ventura R Alternative Long-Term Markers for the Detection of Methyltestosterone Misuse. Steroids. 2013, 78 (1), 44–52. 10.1016/j.steroids.2012.10.008 [PubMed: 23127819]

(6). Gomez C; Fabregat A; Pozo ÓJ; Marcos J; Segura J; Ventura R Analytical Strategies Based on Mass Spectrometric Techniques for the Study of Steroid Metabolism. TrAC - Trends Anal. Chem 2014, 53, 106–116. 10.1016/j.trac.2013.08.010

(7). Narciso J; Luz S; Bettencourt Da Silva R Assessment of the Quality of Doping Substances Identification in Urine by GC/MS/MS. Anal. Chem 2019, 91 (10), 6638–6644. 10.1021/acs.analchem.9b00560 [PubMed: 31016967]

(8). Pozo OJ; Van Eenoo P; Deventer K; Delbeke FT Ionization of Anabolic Steroids by Adduct Formation in Liquid Chromatography Electrospray Mass Spectrometry. J. Mass Spectrom 2007, 42 (4), 497–516. 10.1002/jms.1182 [PubMed: 17328094]

(9). Rannulu NS; Cole RB Novel Fragmentation Pathways of Anionic Adducts of Steroids Formed by Electrospray Anion Attachment Involving Regioselective Attachment, Regiospecific Decompositions, Charge-Induced Pathways, and Ion-Dipole Complex Intermediates. J. Am. Soc. Mass Spectrom 2012, 23 (9), 1558–1568. 10.1007/s13361-012-0422-y [PubMed: 22733166]

(10). Forsdahl G; Zanitzer K; Erceg D; Gmeiner G Quantification of Endogenous Steroid Sulfates and Glucuronides in Human Urine after Intramuscular Administration of Testosterone Esters. Steroids. 2020, 157, 108614. 10.1016/j.steroids.2020.108614 [PubMed: 32097612]

(11). Balcells G; Pozo OJ; Esquivel A; Kotronoulas A; Joglar J; Segura J; Ventura R Screening for Anabolic Steroids in Sports: Analytical Strategy Based on the Detection of Phase I and

Phase II Intact Urinary Metabolites by Liquid Chromatography Tandem Mass Spectrometry. J. Chromatogr. A 2015, 1389, 65–75. 10.1016/j.chroma.2015.02.022 [PubMed: 25746760]

(12). Fabregat A; Pozo OJ; Marcos J; Segura J; Ventura R Use of LC-MS/MS for the Open Detection of Steroid Metabolites Conjugated with Glucuronic Acid. Anal. Chem 2013, 85 (10), 5005–5014. 10.1021/ac4001749 [PubMed: 23586472]

(13). Lee SH; Lee N; Hong Y; Chung BC; Choi MH Simultaneous Analysis of Free and Sulfated Steroids by Liquid Chromatography/Mass Spectrometry with Selective Mass Spectrometric Scan Modes and Polarity Switching. Anal. Chem 2016, 88 (23), 11624–11630. 10.1021/acs.analchem.6b03183 [PubMed: 27934105]

(14). Kotronoulas A; Gomez-Gomez A; Segura J; Ventura R; Joglar J; Pozo OJ Evaluation of Two Glucuronides Resistant to Enzymatic Hydrolysis as Markers of Testosterone Oral Administration. J. Steroid Biochem. Mol. Biol 2017, 165, 212–218. 10.1016/j.jsbmb.2016.06.006 [PubMed: 27328448]

(15). Athanasiadou I; Angelis YS; Lyris E; Georgakopoulos C Chemical Derivatization to Enhance Ionization of Anabolic Steroids in LC-MS for Doping-Control Analysis. TrAC – Trends Anal. Chem 2013, 42, 137–156. 10.1016/j.trac.2012.10.003

(16). Thevis M; Walpurgis K; Thomas A Analytical Approaches in Human Sports Drug Testing: Recent Advances, Challenges, and Solutions. Anal. Chem 2019, 92 (1), 506–523 10.1021/acs.analchem.9b04639 [PubMed: 31610649]

(17). Sobolevsky T; Rodchenkov G Detection and Mass Spectrometric Characterization of Novel Long-Term Dehydrochloromethyltestosterone Metabolites in Human Urine. J. Steroid Biochem. Mol. Biol 2012, 128, 121–127. 10.1016/j.jsbmb.2011.11.004 [PubMed: 22142641]

(18). Kratena N; Enev VS; Gmeiner G; Gärtner P Synthesis of 17β-Hydroxymethyl-17α-Methyl-18-Norandrosta-1,4,13-Trien-3-One: A Long-Term Metandienone Metabolite. Steroids, 2016, 115, 75–79. 10.1016/j.steroids.2016.08.013 [PubMed: 27553728]

(19). Forsdahl G; Geisendorfer T; Göschl L; Pfeffer S; Gärtner P; Thevis M; Gmeiner G Unambiguous Identification and Characterization of a Long-Term Human Metabolite of Dehydrochloromethyltestosterone. Drug Test. Anal 2018, 10 (8), 1244–1250. 10.1002/dta.2385

(20). Liu J; Chen L; Joseph JF; Naß A; Stoll A; de la Torre X; Botrè F; Wolber G; Parr MK; Bureik M Combined Chemical and Biotechnological Production of 20βOH-NorDHCMT, a Long-Term Metabolite of Oral-Turinabol (DHCMT). J. Inorg. Biochem 2018, 183, 165–171. 10.1016/j.jinorgbio.2018.02.020 [PubMed: 29544993]

(21). Kratena N; Pilz SM; Weil M; Gmeiner G; Enev VS; Gärtner P Synthesis and Structural Elucidation of a Dehydrochloromethyltestosterone Metabolite. Org. Biomol. Chem 2018, 16 (14), 2508–2521. 10.1039/c8ob00122g [PubMed: 29565074]

(22). Balcells G; Pozo OJ; Garrostas L; Esquivel A; Matabosch X; Kotronoulas A; Joglar J; Ventura R Detection and Characterization of Clostebol Sulfate Metabolites in Caucasian Population. J. Chromatogr. B Anal. Technol. Biomed. Life Sci 2016, 1022, 54–63. 10.1016/j.jchromb.2016.03.028

(23). Polet M; Van Gansbeke W; Albertsdóttir AD; Coppieters G; Deventer K; Van Eenoo P Gas Chromatography–mass Spectrometry Analysis of Non-Hydrolyzed Sulfated Steroids by Degradation Product Formation. Drug Test. Anal 2019, 11 (11–12), 1656–1665. 10.1002/dta.2606 [PubMed: 31009554]

(24). Hernández-Mesa M; Le Bizec B; Monteau F; García-Campaña AM; Dervilly-Pinel G Collision Cross Section (CCS) Database: An Additional Measure to Characterize Steroids. Anal. Chem 2018, 90 (7), 4616–4625. 10.1021/acs.analchem.7b05117 [PubMed: 29528626]

(25). Gouveia MJ; Brindley PJ; Santos LL; Correia Da Costa JM; Gomes P; Vale N Mass Spectrometry Techniques in the Survey of Steroid Metabolites as Potential Disease Biomarkers: A Review. Metabolism: Clinical and Experimental. 2013, 62 (9), 1206–1217. 10.1016/j.metabol.2013.04.003 [PubMed: 23664145]

(26). Polet M; Van Gansbeke W; Geldof L; Deventer K; Van Eenoo P Identification and Characterization of Novel Long-Term Metabolites of Oxymesterone and Mesterolone in Human Urine by Application of Selected Reaction Monitoring GC-CI-MS/MS. Drug Test. Anal 2017, 9 (11–12), 1673–1684. 10.1002/dta.2183 [PubMed: 28296258]

(27). Wang Z; Zhou X; Liu X; Dong Y; Zhang J A Novel HPLC-MRM Strategy to Discover Unknown and Long-Term Metabolites of Stanozolol for Expanding Analytical Possibilities in Doping-Control. J. Chromatogr. B Anal. Technol. Biomed. Life Sci 2017, 1040, 250–259. 10.1016/j.jchromb.2016.11.006

(28). Balcells G; Matabosch X; Ventura R Detection of Stanozolol O- and N-Sulfate Metabolites and Their Evaluation as Additional Markers in Doping Control. Drug Test. Anal 2017, 9 (7), 1001–1010. 10.1002/dta.2107 [PubMed: 27714936]

(29). Rzeppa S; Viet L Analysis of Sulfate Metabolites of the Doping Agents Oxandrolone and Danazol Using High Performance Liquid Chromatography Coupled to Tandem Mass Spectrometry. J. Chromatogr. B Anal. Technol. Biomed. Life Sci 2016, 1029–1030, 1–9. 10.1016/j.jchromb.2016.06.028

(30). World Anti-Doping Agency (WADA) 2018 Anti-Doping Testing Figures https://www.wada-ama.org/sites/default/files/resources/files/2018_testing_figures_report.pdf

(31). Liu Y; Lu J; Yang S; Zhang Q; Xu Y New Drostanolone Metabolites in Human Urine by Liquid Chromatography Time-of-Flight Tandem Mass Spectrometry and Their Application for Doping Control. Steroids 2016, 108, 61–67. 10.1016/j.steroids.2016.01.013 [PubMed: 26826321]

(32). Piper T; Schänzer W; Thevis M Revisiting the Metabolism of 19-Nortestosterone Using Isotope Ratio and High Resolution/High Accuracy Mass Spectrometry. J. Steroid Biochem. Mol. Biol 2016, 162, 80–91. 10.1016/j.jsbmb.2015.12.013 [PubMed: 26699683]

(33). World Anti-Doping Agency (WADA) Technical Letter 21: In Situ Formation of 4-Androstene-3,6,17-Trione (6-oxo) and Metabolites https://www.wada-ama.org/sites/default/files/resources/files/tl21_6oxo.pdf

(34). Polet M; Van Gansbeke W; Van Eenoo P; Deventer K Efficient Approach for the Detection and Identification of New Androgenic Metabolites by Applying SRM GC-CI-MS/MS: A Methandienone Case Study. J. Mass Spectrom 2016, 51 (7) 524–534. 10.1002/jms.3781 [PubMed: 27434811]

(35). Polet M; Van Gansbeke W; Van Eenoo P; Deventer K Gas Chromatography/Chemical Ionization Triple Quadrupole Mass Spectrometry Analysis of Anabolic Steroids: Ionization and Collision-Induced Dissociation Behavior. Rapid Commun. Mass Spectrom 2016, 30 (4), 511–522. 10.1002/rcm.7472 [PubMed: 26777682]

(36). Marcos J; Pozo OJ Derivatization of Steroids in Biological Samples for GC-MS and LC-MS Analyses. Bioanalysis. 2015, 7 (19), 2515–2536. 10.4155/bio.15.176 [PubMed: 26478271]

(37). Nicoli R; Guillarme D; Leuenberger N; Baume N; Robinson N; Saugy M; Veuthey JL Analytical Strategies for Doping Control Purposes: Needs, Challenges, and Perspectives. Anal. Chem 2016, 88 (1), 508–523. 10.1021/acs.analchem.5b03994 [PubMed: 26566004]

(38). Dodds JN; Hopkins ZR; Knappe DRU; Baker ES Rapid Characterization of Per- And Polyfluoroalkyl Substances (PFAS) by Ion Mobility Spectrometry-Mass Spectrometry (IMS-MS). Anal. Chem 2020, 92 (6), 4427–4435. 10.1021/acs.analchem.9b05364 [PubMed: 32011866]

(39). Viehland LA; Mason EA Gaseous Lon Mobility in Electric Fields of Arbitrary Strength. Ann. Phys 1975, 91 (2), 499–533. 10.1016/0003-4916(75)90233-X

(40). Giles K; Williams JP; Campuzano I Enhancements in Travelling Wave Ion Mobility Resolution. Rapid Communications in Mass Spectrometry. 2011, 25 (11), 1559–1566. 10.1002/rcm.5013 [PubMed: 21594930]

(41). Pu Y; Ridgeway ME; Glaskin RS; Park MA; Costello CE; Lin C Separation and Identification of Isomeric Glycans by Selected Accumulation-Trapped Ion Mobility Spectrometry-Electron Activated Dissociation Tandem Mass Spectrometry. Anal. Chem 2016, 88 (7), 3440–3443. 10.1021/acs.analchem.6b00041 [PubMed: 26959868]

(42). Bijlsma L; Berntssen MHG; Merel S A Refined Nontarget Workflow for the Investigation of Metabolites through the Prioritization by in Silico Prediction Tools. Anal. Chem 2019, 91 (9), 6321–6328. 10.1021/acs.analchem.9b01218 [PubMed: 30973697]

(43). Poland JC; Schrimpe-Rutledge AC; Sherrod SD; Flynn CR; McLean JA Utilizing Untargeted Ion Mobility-Mass Spectrometry to Profile Changes in the Gut Metabolome Following Biliary

Diversion Surgery. Anal. Chem 2019. 91 (22), 14417–14423. 10.1021/acs.analchem.9b02924 [PubMed: 31573190]

(44). May JC; Goodwin CR; Lareau NM; Leaptrot KL; Morris CB; Kurulugama RT; Mordehai A; Klein C; Barry W; Darland E; Overney G; Imatani K; Stafford GC; Fjeldsted JC; McLean JA Conformational Ordering of Biomolecules in the Gas Phase: Nitrogen Collision Cross Sections Measured on a Prototype High Resolution Drift Tube Ion Mobility-Mass Spectrometer. Anal. Chem 2014, 86 (4), 2107–2116. 10.1021/ac4038448 [PubMed: 24446877]

(45). May JC; Dodds JN; Kurulugama RT; Stafford GC; Fjeldsted JC; McLean JA Broadscale Resolving Power Performance of a High Precision Uniform Field Ion Mobility-Mass Spectrometer. Analyst. 2015, 140 (20), 6824–6833. 10.1039/c5an00923e [PubMed: 26191544]

(46). Stow SM; Causon TJ; Zheng X; Kurulugama RT; Mairinger T; May JC; Rennie EE; Baker ES; Smith RD; McLean JA; Hann S; Fjeldsted JC An Interlaboratory Evaluation of Drift Tube Ion Mobility-Mass Spectrometry Collision Cross Section Measurements. Anal. Chem 2017, 89 (17), 9048–9055. 10.1021/acs.analchem.7b01729 [PubMed: 28763190]

(47). Dodds JN; May JC; McLean JA Investigation of the Complete Suite of the Leucine and Isoleucine Isomers: Toward Prediction of Ion Mobility Separation Capabilities. Anal. Chem 2017, 89 (1), 952–959. 10.1021/acs.analchem.6b04171 [PubMed: 28029037]

(48). Nichols CM; Dodds JN; Rose BS; Picache JA; Morris CB; Codreanu SG; May JC; Sherrod SD; McLean JA Untargeted Molecular Discovery in Primary Metabolism: Collision Cross Section as a Molecular Descriptor in Ion Mobility-Mass Spectrometry. Anal. Chem 2018, 90 (24), 14484–14492. 10.1021/acs.analchem.8b04322 [PubMed: 30449086]

(49). Picache JA; Rose BS; Balinski A; Leaptrot KL; Sherrod SD; May JC; McLean JA Collision Cross Section Compendium to Annotate and Predict Multi-Omic Compound Identities. Chem. Sci 2019, 10 (4), 983–993. 10.1039/c8sc04396e [PubMed: 30774892]

(50). May JC; McLean JA Ion Mobility-Mass Spectrometry: Time-Dispersive Instrumentation. Anal. Chem 2015, 87 (3), 1422–1436. 10.1021/ac504720m [PubMed: 25526595]

(51). Leaptrot KL; May JC; Dodds JN; McLean JA Ion Mobility Conformational Lipid Atlas for High Confidence Lipidomics. Nat. Commun 2019, 10 (1), 1–9. 10.1038/s41467-019-08897-5 [PubMed: 30602773]

(52). Chouinard CD; Wei MS; Beekman CR; Kemperman RHJ; Yost RA Ion Mobility in Clinical Analysis: Current Progress and Future Perspectives. Clinical Chemistry. 2016, 62 (1), 124–133. 10.1373/clinchem.2015.238840 [PubMed: 26585928]

(53). Harris RA; Leaptrot KL; May JC; McLean JA New Frontiers in Lipidomics Analyses Using Structurally Selective Ion Mobility-Mass Spectrometry. TrAC - Trends Anal. Chem 2019, 116, 316–323. 10.1016/j.trac.2019.03.031

(54). Maddox SW; Fraser Caris RH; Baker KL; Burkus-Matesevac A; Peverati R; Chouinard CD Ozone-Induced Cleavage of Endocyclic C═C Double Bonds within Steroid Epimers Produces Unique Gas-Phase Conformations. J. Am. Soc. Mass Spectrom 2020, 31 (2), 411–417. 10.1021/jasms.9b00058 [PubMed: 32031388]

(55). Harris RA; May JC; Stinson CA; Xia Y; McLean JA Determining Double Bond Position in Lipids Using Online Ozonolysis Coupled to Liquid Chromatography and Ion Mobility-Mass Spectrometry. Anal. Chem 2018, 90 (3), 1915–1924. 10.1021/acs.analchem.7b04007 [PubMed: 29341601]

(56). Sherrod SD; McLean JA Systems-Wide High-Dimensional Data Acquisition and Informatics Using Structural Mass Spectrometry Strategies. Clinical Chemistry. 2016, 62 (1), 77–83. 10.1373/clinchem.2015.238261 [PubMed: 26453699]

(57). Schrimpe-Rutledge AC; Codreanu SG; Sherrod SD; McLean JA Untargeted Metabolomics Strategies—Challenges and Emerging Directions. J. Am. Soc. Mass Spectrom 2016, 27 (12), 1897–1905. 10.1007/s13361-016-1469-y [PubMed: 27624161]

(58). Gabelica V; Shvartsburg AA; Afonso C; Barran P; Benesch JLP; Bleiholder C; Bowers MT; Bilbao A; Bush MF; Campbell JL; Campuzano IDG; Causon T; Clowers BH; Creaser CS; De Pauw E; Far J; Fernandez-Lima F; Fjeldsted JC; Giles K; Groessl M; Hogan CJ; Hann S; Kim HI; Kurulugama RT; May JC; McLean JA; Pagel K; Richardson K; Ridgeway ME; Rosu F; Sobott F; Thalassinos K; Valentine SJ; Wyttenbach T Recommendations for Reporting

Ion Mobility Mass Spectrometry Measurements. Mass Spectrom. Rev 2019, 38 (3), 291–320. 10.1002/mas.21585 [PubMed: 30707468]

(59). Dodds JN; Baker ES Ion Mobility Spectrometry: Fundamental Concepts, Instrumentation, Applications, and the Road Ahead. J. Am. Soc. Mass Spectrom 2019, 30 (11), 2185–2195. 10.1007/s13361-019-02288-2 [PubMed: 31493234]

(60). Hines KM; Ballard BR; Marshall DR; McLean JA Structural Mass Spectrometry of Tissue Extracts to Distinguish Cancerous and Non-Cancerous Breast Diseases. Mol. Biosyst 2014, 10 (11), 2827–2837. 10.1039/c4mb00250d [PubMed: 25212505]

(61). Fenn LS; McLean JA Biomolecular Structural Separations by Ion Mobility-Mass Spectrometry. Anal. Bioanal. Chem 2008, 391 (3), 905–909. 10.1007/s00216-008-1951-x [PubMed: 18320175]

(62). Goodwin CR; Fenn LS; Derewacz DK; Bachmann BO; McLean JA Structural Mass Spectrometry: Rapid Methods for Separation and Analysis of Peptide Natural Products. J. Nat. Prod 2012, 75 (1), 48–53. 10.1021/np200457r [PubMed: 22216918]

(63). Hines KM; Ross DH; Davidson KL; Bush MF; Xu L Large-Scale Structural Characterization of Drug and Drug-Like Compounds by High-Throughput Ion Mobility-Mass Spectrometry. Anal. Chem 2017, 89 (17), 9023–9030. 10.1021/acs.analchem.7b01709 [PubMed: 28764324]

(64). Mairinger T; Causon TJ; Hann S The Potential of Ion Mobility–Mass Spectrometry for Non-Targeted Metabolomics. Curr. Opin. Chem. Biol 2018, 42, 9–15. 10.1016/j.cbpa.2017.10.015 [PubMed: 29107931]

(65). Zhang X; Quinn K; Cruickshank-Quinn C; Reisdorph R; Reisdorph N The Application of Ion Mobility Mass Spectrometry to Metabolomics. Current Opinion in Chemical Biology. 2018, 42, 60–66. 10.1016/j.cbpa.2017.11.001 [PubMed: 29161611]

(66). May JC; Gant-Branum RL; McLean JA Targeting the Untargeted in Molecular Phenomics with Structurally-Selective Ion Mobility-Mass Spectrometry. Current Opinion in Biotechnology. 2016, 39, 192–197. 10.1016/j.copbio.2016.04.013 [PubMed: 27132126]

(67). Maddox SW; Olsen SSH; Velosa DC; Burkus-Matesevac A; Peverati R; Chouinard CD Improved Identification of Isomeric Steroids Using the Paternò-Büchi Reaction with Ion Mobility-Mass Spectrometry. J. Am. Soc. Mass Spectrom 2020, 31 (10), 2086–2092. 10.1021/jasms.0c00215 [PubMed: 32870679]

(68). Hernández-Mesa M; D'Atri V; Barknowitz G; Fanuel M; Pezzatti J; Dreolin N; Ropartz D; Monteau F; Vigneau E; Rudaz S; Stead S; Rogniaux H; Guillarme D; Dervilly G; Le Bizec B Interlaboratory and Interplatform Study of Steroids Collision Cross Section by Traveling Wave Ion Mobility Spectrometry. Anal. Chem 2020, 92 (7), 5013–5022. 10.1021/acs.analchem.9b05247 [PubMed: 32167758]

(69). Hernández-Mesa M; Monteau F; Le Bizec B; Dervilly-Pinel G Potential of Ion Mobility-Mass Spectrometry for Both Targeted and Non-Targeted Analysis of Phase II Steroid Metabolites in Urine. Anal. Chim. Acta X 2019, 1. 10.1016/j.acax.2019.100006

(70). Chouinard CD; Cruzeiro VWD; Roitberg AE; Yost RA Experimental and Theoretical Investigation of Sodiated Multimers of Steroid Epimers with Ion Mobility-Mass Spectrometry. J. Am. Soc. Mass Spectrom 2017, 28 (2), 323–331. 10.1007/s13361-016-1525-7 [PubMed: 27914014]

(71). Wei MS; Kemperman RHJ; Palumbo MA; Yost RA Separation of Structurally Similar Anabolic Steroids as Cation Adducts in FAIMS-MS. J. Am. Soc. Mass Spectrom 2020, 31 (2), 355–365. 10.1021/jasms.9b00127 [PubMed: 32031405]

(72). Plachká K; Pezzatti J; Musenga A; Nicoli R; Kuuranne T; Rudaz S; Nováková L; Guillarme D Ion Mobility-High Resolution Mass Spectrometry in Anti-Doping Analysis. Part I: Implementation of a Screening Method with the Assessment of a Library of Substances Prohibited in Sports. Anal. Chim. Acta 2021, 1152. 10.1016/j.aca.2021.338257

(73). Cumeras R; Figueras E; Davis CE; Baumbach JI; Gràcia I Review on Ion Mobility Spectrometry. Part 1: Current Instrumentation. Analyst. 2015, 140 (5), 1376–1390. 10.1039/c4an01100g [PubMed: 25465076]

(74). Cumeras R; Figueras E; Davis CE; Baumbach JI; Gràcia I Review on Ion Mobility Spectrometry. Part 2: Hyphenated Methods and Effects of Experimental Parameters. Analyst. 2015, 140 (5), 1391–1410. 10.1039/c4an01101e [PubMed: 25465248]

(75). Davis DE; Sherrod SD; Gant-Branum RL; Colby JM; McLean JA Targeted Strategy to Analyze Antiepileptic Drugs in Human Serum by LC-MS/MS and LC-Ion Mobility-MS. Anal. Chem 2020, 92 (21), 14648–14656. 10.1021/acs.analchem.0c03172 [PubMed: 33047601]

(76). May JC; Goodwin CR; McLean JA Ion Mobility-Mass Spectrometry Strategies for Untargeted Systems, Synthetic, and Chemical Biology. Current Opinion in Biotechnology. 2015, 31, 117–121. 10.1016/j.copbio.2014.10.012 [PubMed: 25462629]

(77). Dodds JN; May JC; McLean JA Correlating Resolving Power, Resolution, and Collision Cross Section: Unifying Cross-Platform Assessment of Separation Efficiency in Ion Mobility Spectrometry. Anal. Chem 2017, 89 (22), 12176–12184. 10.1021/acs.analchem.7b02827 [PubMed: 29039942]

(78). May JC; McLean JA Advanced Multidimensional Separations in Mass Spectrometry: Navigating the Big Data Deluge. Annu. Rev. Anal. Chem 2016, 9 (1), 387–409. 10.1146/annurev-anchem-071015-041734

(79). MacLean B; Finney GL; Chambers M; MacCoss MJ; Liebler DC; Shulman N; Tomazela DM; Tabb DL; Kern R; Frewen B; et al. Skyline: An Open Source Document Editor for Creating and Analyzing Targeted Proteomics Experiments. Bioinformatics. 2010, 26 (7), 966–968. 10.1093/bioinformatics/btq054 [PubMed: 20147306]

(80). Henderson CM; Shulman NJ; MacLean B; MacCoss MJ; Hoofnagle AN Skyline Performs as Well as Vendor Software in the Quantitative Analysis of Serum 25-Hydroxy Vitamin D and Vitamin D Binding Globulin. Clin. Chem 2017, 64 (2), 408–410. 10.1373/clinchem.2017.282293 [PubMed: 29203474]

(81). Giles K; Ujma J; Wildgoose J; Pringle S; Richardson K; Langridge D; Green MA Cyclic Ion Mobility-Mass Spectrometry System. Anal. Chem 2019, 91 (13), 8564–8573. 10.1021/acs.analchem.9b01838 [PubMed: 31141659]

(82). May JC; Knochenmuss R; Fjeldsted JC; McLean JA Resolution of Isomeric Mixtures in Ion Mobility Using a Combined Demultiplexing and Peak Deconvolution Technique. Anal. Chem 2020, 92 (14), 9482–9492. 10.1021/acs.analchem.9b05718 [PubMed: 32628451]

(83). Kirk AT; Bohnhorst A; Raddatz CR; Allers M; Zimmermann S Ultra-High-Resolution Ion Mobility Spectrometry—Current Instrumentation, Limitations, and Future Developments. Analytical and Bioanalytical Chemistry. 2019, 411 (24), 6229–6246. 10.1007/s00216-019-01807-0 [PubMed: 30957205]

(84). Hollerbach AL; Li A; Prabhakaran A; Nagy G; Harrilal CP; Conant CR; Norheim RV; Schimelfenig CE; Anderson GA; Garimella SVB; Smith RD; Ibrahim YM Ultra-High-Resolution Ion Mobility Separations over Extended Path Lengths and Mobility Ranges Achieved Using a Multilevel Structures for Lossless Ion Manipulations Module. Anal. Chem 2020, 92 (11), 7972–7979. 10.1021/acs.analchem.0c01397 [PubMed: 32383592]

(85). Deng L; Ibrahim YM; Hamid AM; Garimella SVB; Webb IK; Zheng X; Prost SA; Sandoval JA; Norheim RV; Anderson GA; Tolmachev AV; Baker ES; Smith RD Ultra-High Resolution Ion Mobility Separations Utilizing Traveling Waves in a 13 m Serpentine Path Length Structures for Lossless Ion Manipulations Module. Anal. Chem 2016, 88 (18), 8957–8964. 10.1021/acs.analchem.6b01915 [PubMed: 27531027]

(86). Ibrahim YM; Hamid AM; Deng L; Garimella SVB; Webb IK; Baker ES; Smith RD New Frontiers for Mass Spectrometry Based upon Structures for Lossless Ion Manipulations. Analyst. 2017, 142 (7), 1010–1021. 10.1039/c7an00031f [PubMed: 28262893]

(87). Esquivel A, Alechaga E, Monfort N, Ventura R: Direct Quantitation of endogenous steroid sulfate in human urine by liquid chromatography-electrospray tandem mass spectrometry. Drug Test Anal. 2018, 10(11-12), 1734–1743. [PubMed: 29797686]

(88). Plante PL; Francovic-Fontaine É; May JC; McLean JA; Baker ES; Laviolette F; Marchand M; Corbeil J Predicting Ion Mobility Collision Cross-Sections Using a Deep Neural Network: DeepCCS. Anal. Chem 2019, 91 (8), 5191–5199. 10.1021/acs.analchem.8b05821 [PubMed: 30932474]

(89). Picache JA, May JC, & McLean JA; Chemical Class Prediction of Unknown Biomolecules Using Ion Mobility-Mass Spectrometry and Machine Learning: Supervised Inference of Feature Taxonomy from Ensemble Randomization. Anal. Chem, 2020, 92(15), 10759–10767.10.1021/acs.analchem.0c02137 [PubMed: 32628452]

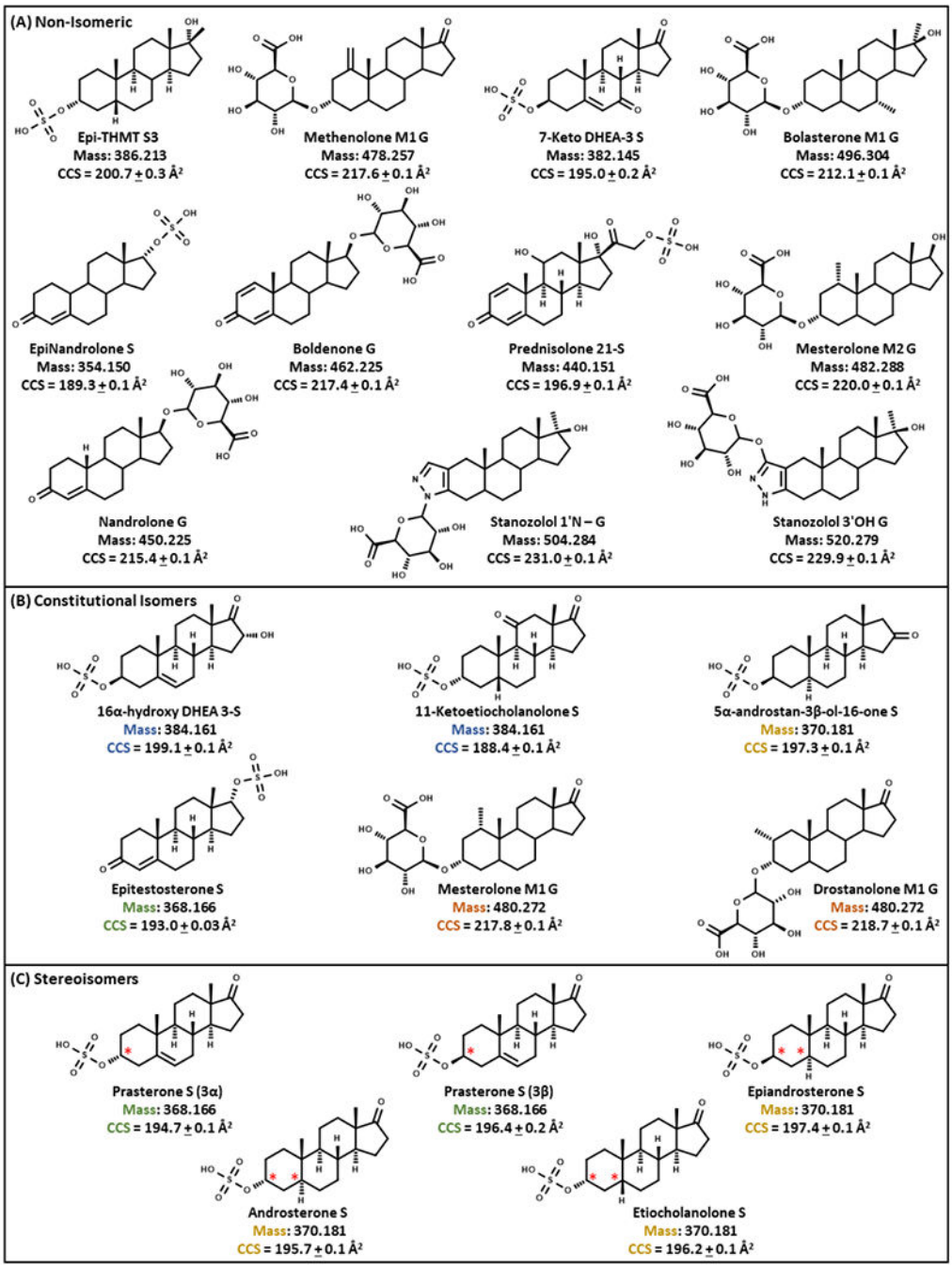

Figure 1.

Chemical structures, exact masses, and CCS values of 22 phase II steroids categorized as (A) non-isomeric, (B) constitu-tional isomers, and (C) stereoisomers. Reported CCS measurements represent $n = 3$ technical replicates over 3 different days at 5 μg/mL. The color coordination is for isomer groups and the red stars indicate positions of stereochemistry that differentiate stereo-isomers.

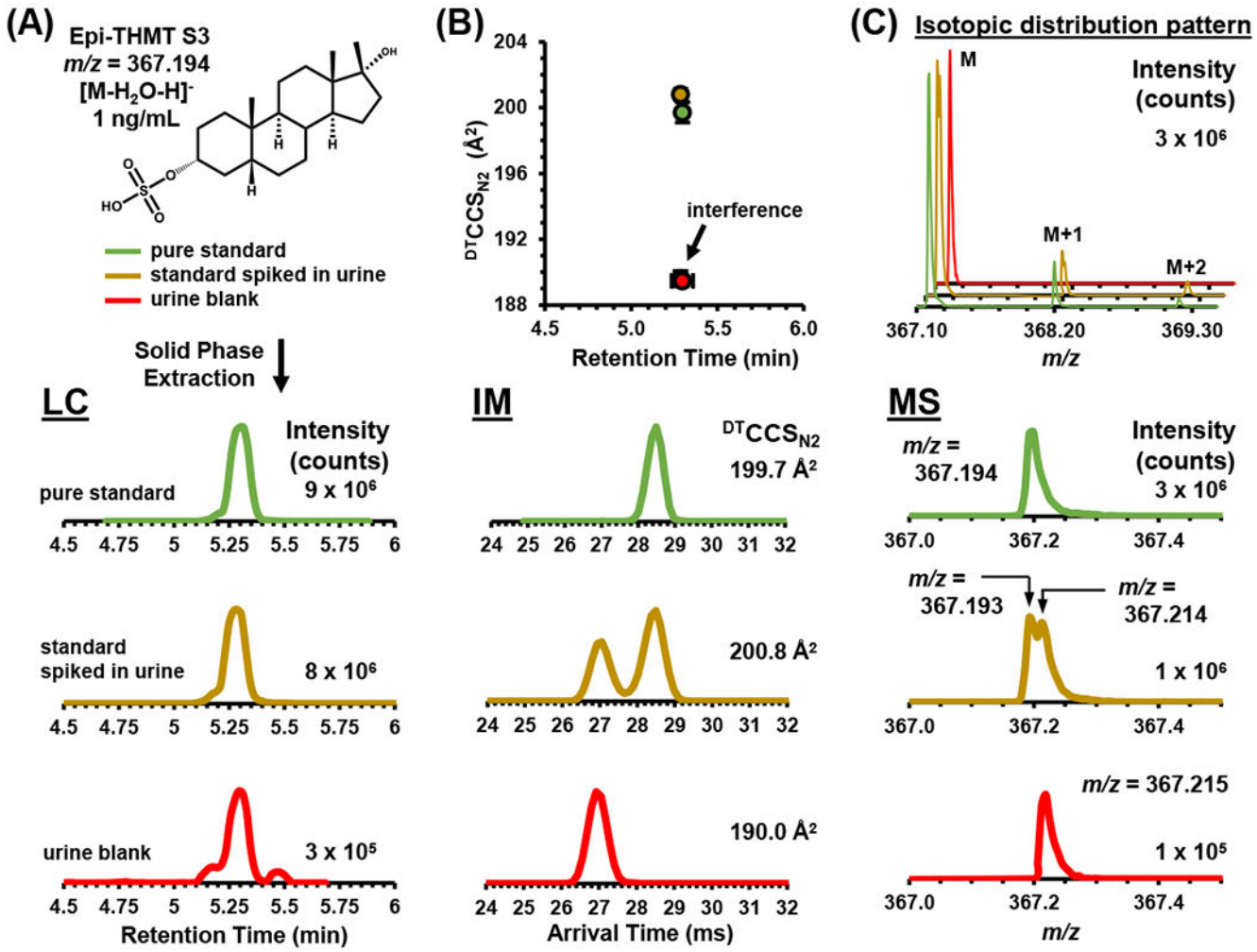

Figure 2.

The anabolic-androgenic steroids (AASs) analytical workflow for the liquid chromatography (LC)-ion mobility (IMS)-mass spectrometry (MS) method with 17-methyltestosterone sulfate metabolite 3 (Epi-THMT S3 as $[M\text{-}H_2O\text{-}H]^-$ found in Figure S1) as an example using the 10 minute LC method (Table S1). (A) EPI-THMT S3's chemical structure, color coordination legend, sample preparation, LC chromatograms relative intensity vs. retention time in minutes (min) as extracted ion chromatograms (EIC) for 367.1930 *m/z*. (B) Comparison of collision cross section (CCS) values vs. retention time (min), drift time relative inten-sity vs. IM spectra in milliseconds (ms). (C) HRMS mass spectra relative intensity vs. *m/z*. In (B) standard error bars were used to demonstrate overlapping CCS values vs. retention times and are within the scale of the marker for most values ($n = 3$ intraday technical replicates).

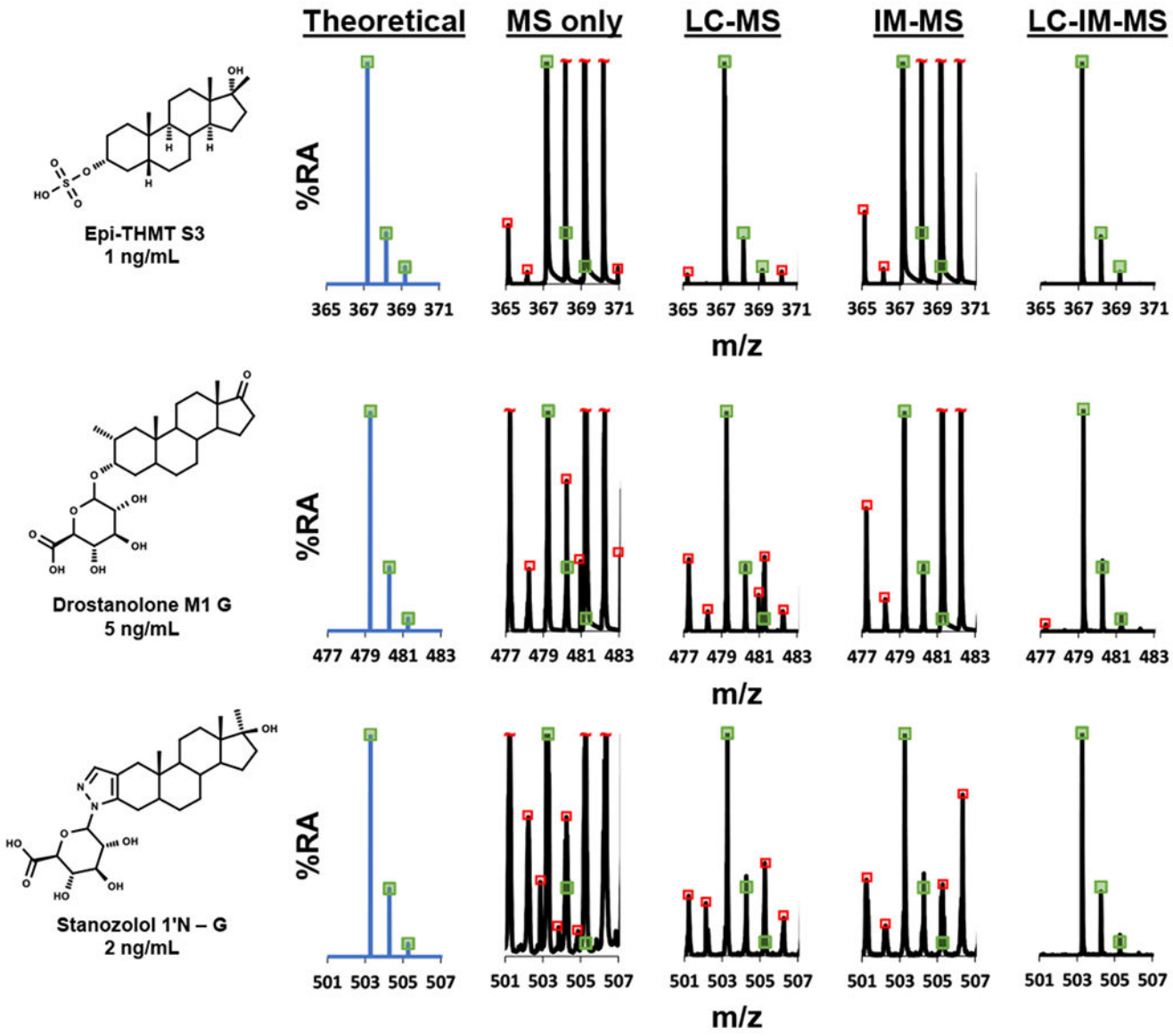

Figure 3.

Isotope distribution patterns for three exogenous AASs (Epi-THMT S3 (World Anti-Doping Agency (WADA) minimum required performance level or MRPL = 2 ng/mL) extracted from human urine samples and analyzed via LC-IM-MS. The mass spectra in this figure are presented as extracted isotopic distribution patterns for the MS only, LC-MS, IM-MS, and LC-IM-MS dimensions. All chromatographic and ion mobility peaks were extracted for the MS only dimension mass spectra. For the LC-MS dimension mass spectra, the AAS chromatographic peaks for Epi-THMT S3, Drostanolone M1 G, and Stanozolol 1'N – G were individually filtered while the entire ion mobility range (0-60 ms) were extracted. For the IM-MS dimension mass spectra, all the chromatographic peaks were extracted while the AAS ion mobility peaks for Epi-THMT S3, Drostanolone M1 G, and Stanozolol 1'N – G were individually filtered. For the LC-IM-MS dimension mass spectra, the AAS chromatographic peaks and ion mobility peaks for Epi-THMT S3, Drostanolone M1 G, and

Stanozolol 1'N – G were individually filtered. This strategy can be used to enhance the confidence in AAS differentiation where the green boxes indicate theoretical mass isotopic distribution matches (±5% height deviation). This figure also presents red boxes that indicate isotopic distribution concomitant interfer-ences that were analyzed in the human urine complex biological sample for the MS only, LC-MS, IM-MS, and LC-IM-MS dimen-sions. In the MS only, LC-MS, and IM-MS dimensions numerous interferences were analyzed. Ultimately, the LC-IM-MS dimen-sion resolved most, if not all, interferences for Epi-THMT S3, Drostanolone M1 G, and Stanozolol 1'N – G. The concept of this figure was in part adapted from Davis, Jr., et al. showing the utility of LC-IM-MS analyses in human urine anti-doping applications.[75]

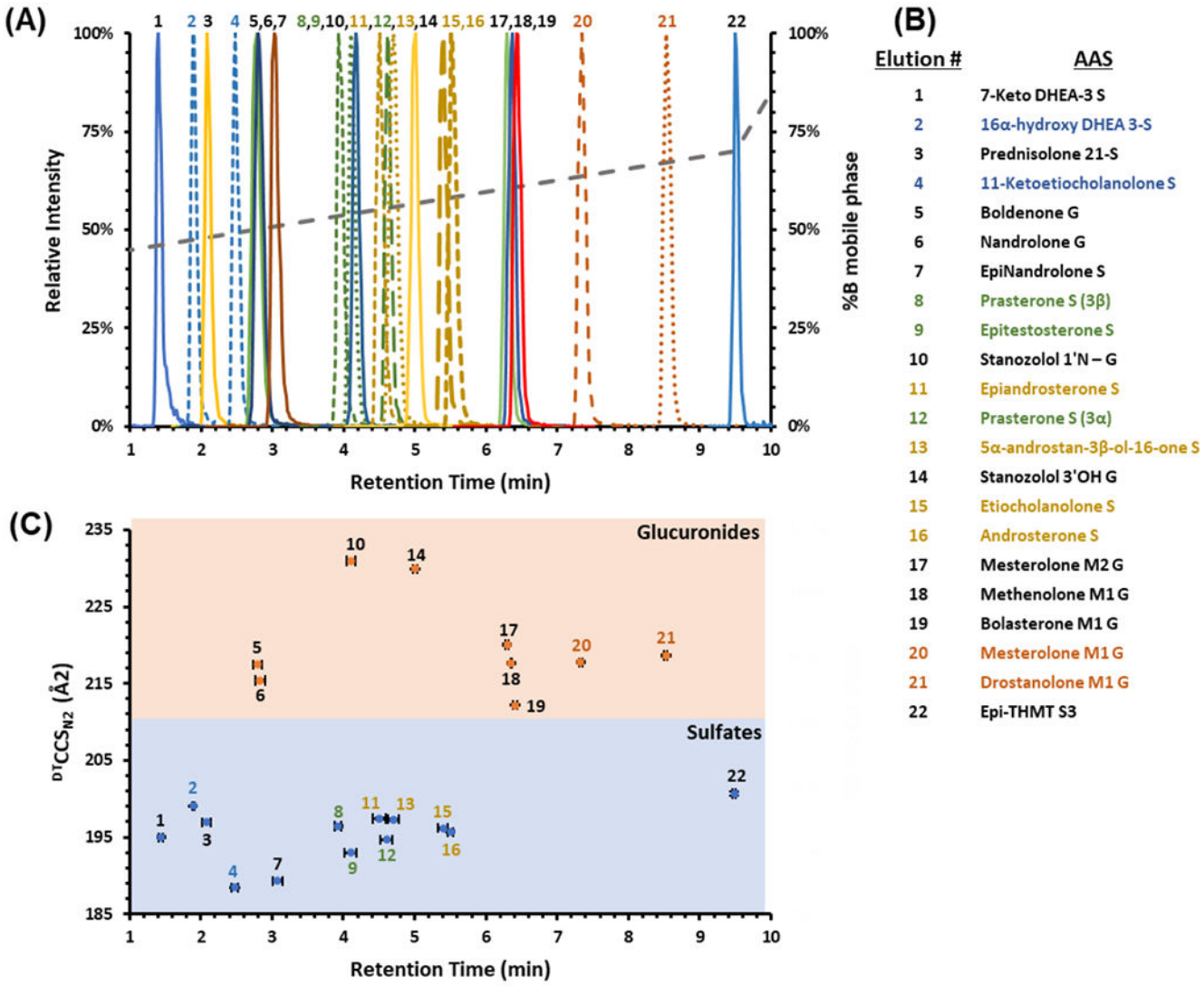

Figure 4.

(A) LC-IMS-MS analysis showing an LC chromatogram of 22 phase II AAS. Dashed chromatograms are isomer groups. The dotted grey line represents %B mobile phase gradient. (B) The elution order of the 22 phase II AAS where the color coordina-tion designates isomer groups. (C) Correlation of LC retention times and CCS values to specific types of phase II steroids (glucuronic acids are in orange and sulfonic acids are in blue). Standard error bars for both variation in retention times and CCS are shown and are for most values within the scale of the marker (n = 3 technical replicates over 3 different days at 5 μg/mL).

Table 1.

AASs separated by isomer groups, neutral formulas, neutral exact mass, adduct exact mass, retention time (RT) using the 15 minute method, elution order annotation, RT CV%, collision cross sections (Å^2), and CCS CV% (n = 3 technical replicates over 3 different days at 5 μg/mL). The color coordination is for isomer types described throughout this manuscript.

AAS	Formula	Exact Mass	$[M-H]^-$	Elution #	RT (min)	RT CV%	CCS	CCS CV%
Epi-THMT S3	$C_{20}H_{34}O_5S$	3S6.213	385.205	22	9.5	0.2	200.7	0.3
Methenolone MlG	$C_{26}H_{38}O_8$	478.257	477.249	18	6.4	0.2	217.6	0.1
7-Keto DHEA-3 S	$C_{19}H_{26}O_6S$	382.145	381.137	1	1.4	2.1	195.0	0.2
Bolasterone Ml G	$C_{27}H_{44}O_8$	496.304	495.296	19	6.4	0.5	212.2	0.1
EpiNandrolone S	$C_{18}H_{26}O_5S$	354.150	353.142	7	3.1	2.3	189.3	0.1
Boldenone G	$C_{25}H_{34}O_5$	462.225	461.218	5	2.8	2.3	217.4	0.1
Prednisolone 21-S	$C_{21}H_{28}O_8S$	440.151	439.143	3	2.1	3.2	196.9	0.1
Mesterolone M2G	$C_{26}H_{42}O_8$	482.288	481.280	17	6.3	0.3	220.0	0.1
Nandrolone G	$C_{24}H_{34}O_8$	450.225	449.218	6	2.8	2.5	215.4	0.1
Stanozolol l'N-G	$C_{19}H_{40}N_2O_7S$	504.284	503.276	10	4.1	1.4	231.0	0.1
Stanozolol 3'OH G	$C_{19}H_{40}N_2O_8S$	520.279	519.271	14	5	0.6	229.9	0.1
Constitutional Isomers								
16α-hydroxy DHEA3-S	$C_{19}H_{28}O_6S$	384.161	383.153	2	1.9	1.0	199.1	0.1
11-Ketoetiocholanolone S	$C_{19}H_{28}O_6S$	384.161	383.153	4	2.5	1.8	188.4	0.1
5α-androstan-3β-ol-16-one S	$C_{19}H_{28}O_5S$	370.181	369.174	13	4.7	1.6	197.3	0.1
EpitestosteroneS	$C_{19}H_{28}O_5S$	368.166	367.158	9	4.1	2.1	193.0	0.03
Mesterolone M1 G	$C_{26}H_{40}O_9$	480.272	479.265	20	7.3	0.3	217.8	0.1
Drostanolone M1 G	$C_{26}H_{40}O_8$	480.272	479.265	21	8.5	0.3	218.7	0.1
Stereoisomers								
Prasterone S (3α)	$C_{19}H_{28}O_5S$	368.166	367.158	12	4.6	1.9	194.7	0.1
Prasterone S (3β)	$C_{19}H_{28}O_5S$	368.166	367.158	8	3.9	1.1	196.4	0.2
Epiandrosterone S	$C_{19}H_{30}O_5S$	370.181	369.174	11	4.5	2.1	197.4	0.1
Androsterone S	$C_{19}H_{30}O_5S$	370.181	369.174	16	5.5	0.6	195.7	0.1
Etiocholanolone S	$C_{19}H_{30}O_5S$	370.181	369.174	15	5.4	1.2	196.2	0.1